GEOLOGICA CARPATHICA, JUNE 2005, 56, 3, 205–221

Exotic orthogneiss pebbles from Paleocene flysch of the Dukla Nappe (Outer Eastern Carpathians, Poland)

KRZYSZTOF BĄK[1] and ANNA WOLSKA[2]

[1]Institute of Geography, Cracow Pedagogical University, Podchorążych 2, 30-084 Kraków, Poland; sgbak@cyf-kr.edu.pl
[2]Institute of Geological Sciences, Jagiellonian University, Oleandry 2a, 30-063 Kraków, Poland; wolska@ing.uj.edu.pl

(Manuscript received December 16, 2003; accepted in revised form September 29, 2004)

Abstract: Crystalline exotic pebbles have been found in the deep-water flysch of the Cisna Beds, in the Dukla Nappe, Polish part of the Outer Western Carpathians. Most of them occur in a layer, which extends over a distance of at least 3 km within the SE limb of the Chryszczata–Wołosań–Mała Rawka anticline. The dimensions of the pebbles vary between 2 and 18 cm (middle axis). The exotic pebbles consist of three types of granite derived orthogneisses: **1** — medium-grained, medium-banded orthogneiss with alkali feldspar porphyroblasts showing structural features of foliated granitic-gneiss, **2** — medium-banded, medium-layered orthogneiss containing small microcline porphyroblasts and showing structural features of foliated granitic-gneiss, and **3** — strongly cataclastic granitic-gneiss with chess-board albite porphyroblasts showing properties of partly mylonitized granite. The chemical composition of the orthogneisses indicates that the protolith was represented by peraluminous, poorly-evolved, S-type granites exhibiting features of orogen-related crustal granites. The discrimination shows that the protolith of the studied rocks evolved in active continental margin or continental collision environments. The biostratigraphical data on deep-water agglutinated Foraminifera suggest the position of the exotic-bearing layer in the lowermost part of the *Rzehakina fissistomata* Zone corresponding to the lowermost Paleocene. Petrographic affinities between orthogneissic pebbles and mineral/rock fragments grains of the Cisna-type sandstones show that they have the same provenance. These deposits were transported from the NE extension of the Marmarosh massif, which had the character of a continental bearing source cordillera, formed mainly by orthogneissic and granitic rocks.

Key words: Paleocene, Outer Carpathians, Dukla Nappe, provenance, stratigraphy, geochemistry, petrography, orthogneissic pebbles.

Introduction

Crystalline exotic pebbles have been found within the thick series of deep-water, Maastrichtian-Paleocene flysch deposits of the Dukla Nappe in the Polish part of the Outer Eastern Carpathians. These flysch series, called the Cisna Beds, belong to the northern part of the Dukla Nappe, outcropping in the Bieszczady Mountains, close to the state boundary between Poland and Ukraine (Fig. 1).

The exotics from the Cisna Beds have not been described in the Polish part of the Dukla Nappe, however, a single bed of gravelstone with quartz, quartzite and phyllite pebbles was noted in Slovakia (Medzilaborce area, Kamjan Mt; Koráb & Ďurkovič 1978).

The exotic rocks, presented here, have been found during geological mapping by the first author (Ustrzyki Górne sheet (1058) for the Detailed Geological Map of Poland, scale 1:50,000; Haczewski et al. submit.). They have been found as loose pebbles in the channels of several left tributaries of the Wołosatka stream in the Bieszczady Mts, Poland. Their abundant occurrences in several neighbouring, parallel creeks suggest the same stratigraphic position of the exotic occurrences.

The aim of this paper is to characterize the exotics and to detect their provenance. Thus the petrographical characteristics obtained for these pebbles are compared with the data from the exotic-bearing layer and surrounding series, as well as with data available in literature. The chemical characteristics of the crystalline exotics and their radiometric age are used to discriminate their protolith.

Geological setting

The described exotic rocks occur in the Dukla Nappe, which belongs to the Fore-Magura group of nappes and is exposed at the surface mainly in the Eastern Carpathians, within the Polish, Slovak and Ukrainian territories.

The studied area occurs to the south of the main overthrust of the Dukla Nappe, in a zone to the south of Ustrzyki Górne village, close to the state boundary with Ukraine (Fig. 1B). The deposits are exposed within the Wołosań–Chryszczata–Mała Rawka anticline, the northernmost tectonic unit of the Dukla Nappe in its Polish part. The NE limb of this fold has been strongly tectonized, contrary to the SW limb (partly in the Ukrainian territory) which presents a continuous section

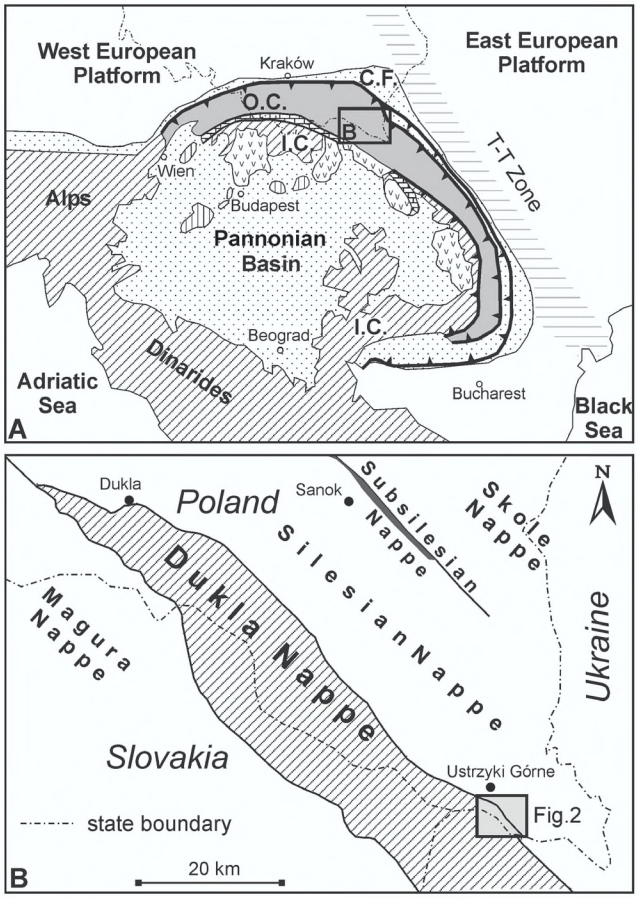

Fig. 1. Position of the studied area in relation to the main geological units. **A** — Outer Carpathians (O.C.) against the background of a simplified geological map of the Alpine orogens and their foreland; I.C. — Inner Carpathians, C.F. — Carpathian Foredeep. **B** — Dukla Nappe against the background of the eastern part of the Outer Carpathians.

(Fig. 2A). The deposits in this limb include Upper Campanian through middle Eocene deep-water flysch strata (Koszarski et al. 1961; Ślączka 1971; Bąk 2004). The lithostratigraphic inventory starts with the Upper Campanian-Maastrichtian Łupków Beds, and includes the Upper Maastrichtian-Paleocene Cisna Beds, the Upper Paleocene Majdan Beds and the uppermost Paleocene-Eocene Hieroglyphic Beds. The total thickness of the Dukla sedimentary sequence reaches 2600 m in the studied part of the Bieszczady Mts.

The described exotic rocks come from the outcrops of the Cisna Beds, which are the thickest unit in this part of the Dukla Nappe (about 1100–1250 m).

The most characteristic feature of the Cisna Beds is the occurrence of grey (grey-brown on weathered surfaces), thick-bedded (even more than 3 m), fine- to coarse-grained, polymictic sandstones with calcareous-siliceous cement (so-called Cisna-type sandstones). The thickness of the thick-bedded sandstone packages reaches up to 50 m; it decreases upwards to a few meters in the uppermost part of the member. Shales are a subordinate component in the Cisna Beds. Most of them are dark grey, black, sandy, non-calcareous shales, occurring in packages 10–40 cm thick.

The thick-bedded packages are intercalated with thin- to medium-, rarely thick-bedded (up to 150 cm; mean — 30–60 cm) sandstones, thin-bedded mudstones and sandy, non-calcareous shales. The grey-yellow colour of weathered surfaces is a very characteristic feature of the sandstone and mudstone beds. The sandstones are medium- to fine-grained, have calcareous or calcareous-siliceous cement, with frequent lamination of various types. The proportion of shales is higher than in the thick-bedded packages, and it increases upwards. The shales are non-calcareous, dark grey, brown, black, and rarely green.

Calcareous spotty marls and calcareous mudstones, 4–7 cm thick, so-called fucoid marls, occur in the upper part of the Cisna Beds. Brown, ferrous coats cover the surface of the marls. The marls occur in packages 40–60 cm thick, together with brown, non-calcareous shales.

Moreover, single beds (30–50 cm thick on average) of grey-green, fine-grained, muscovite-rich, siliceous sandstones occur in the upper part of the Cisna Beds. Abundant plant detritus covers their upper surfaces.

Localities with exotic rocks

Most exotic pebbles have been found in the bedrock of five parallel creeks (Fig. 2A), left tributaries of the Wołosatka stream, which cross the SE limb of the Chryszczata–Wołosań–Mała Rawka anticline. Most pebbles have been found in the upper reaches of the creeks, along a straight line parallel to the local structural grain. The exotic-bearing layer does not outcrop there from beneath the thick alluvium in these sections of the creeks. The supposed position of the exotic-bearing layer is marked there by the occurrence of numerous crystalline pebbles over small alluvial sections of the creeks (ca. 5–10 pebbles per 10 square meters). Additionally, no exotic pebbles have been found in the higher parts of the creeks, where the bedrock is exposed over a distance of at least 100–200 m.

Several exotic pebbles and a block of sandstone with exotic pebbles have been also found in other creeks, located west of the Semenowa Mount. This area also lies within the SE limb of the Chryszczata–Wołosań–Mała Rawka anticline. The exotic finds in individual creeks are not aligned; hence the position of the supposed exotic-bearing layer has not been established there.

The first author collected dozens of exotic pebbles from the described outcrops. Their dimensions vary between 2 and 18 cm (middle axis), 3–10 cm on average. The largest of the exotic clasts, found in the Szczawianka creek measured 20×18×12 cm.

The exotic-bearing layer has not been found *in situ* but a fragment of a sandstone bed (30×15×7 cm) with gneissic clasts (Fig. 3.1), found as a loose block in the Semenowa creek, has been accepted as a sample of this bed.

The exotic pebbles have various degrees of roundness, generally moderate to high. Their roundness is probably original, as indicated by the pebbles in the mentioned fragment of the sandstone bed with clasts (cf. Fig. 3.1).

Taking into account the dips of the beds, the stratigraphic position of the supposed exotic-bearing layer occurs 550 m

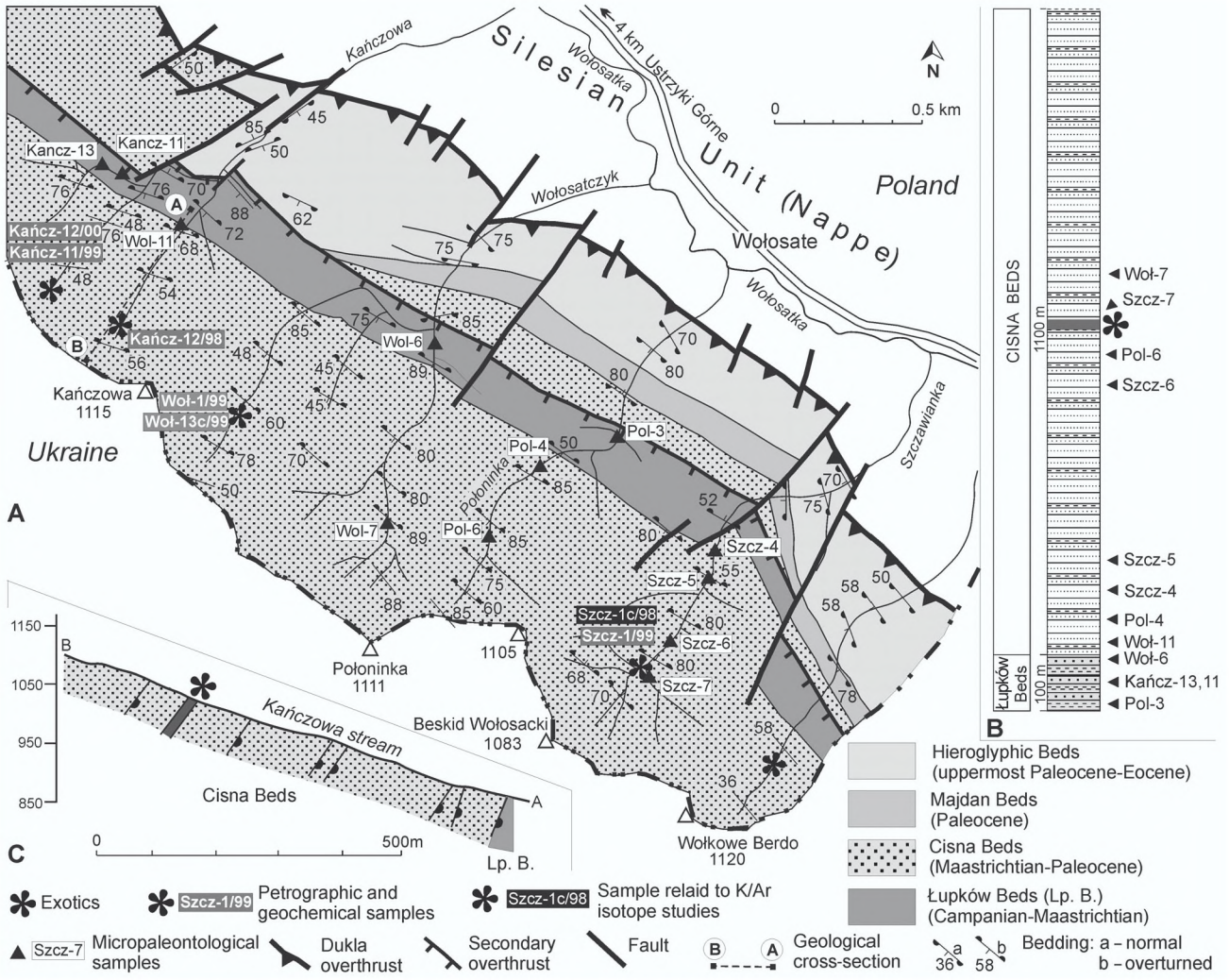

Fig. 2. **A** — Geological map of the Dukla Nappe in the Wołosatka drainge basin (Bieszczady Mts, Poland) with suggested position of the exotic-bearing layer (map after Bąk in Haczewski et al. submit.). **B** — Lithological profile of the Łupków Beds and the Cisna Beds in the studied area, with suggested position of the exotic-bearing layer and position of micropaleontological samples. **C** — Geological cross-section along the Kańczowa stream with suggested position of the exotic-bearing layer.

above the base of the Cisna Beds (Fig. 2B–C). The same position in the parallel creeks may suggest that the layer represents a continuous horizon, at least 3 km long within the southern limb of the Wołosań–Chryszczata–Mała Rawka anticline.

Methods of investigations

The JEOL 5410 electron microscope equipped with an energy spectrometer Voyager 3100 (NORAN) was used to microprobe chemical analyses of rock-forming minerals. The measurements were carried out using a spot method. Samples representing three types of gneissic pebbles (Szcz-1/99, Woł-13c/99 and Kańcz-12/98) were analysed in the Activation Laboratories Ltd. in Canada by means of the following geochemical methods: ICP (major elements), INAA (trace elements including REE) and XRF (Nb). The largest pebble (Szcz-1c/98) was relaid to K/Ar isotope studies (for details see Poprawa et al. 2004).

The foraminiferal samples were collected from exposures of the uppermost part of the Łupków Beds and a lower part of the Cisna Beds, along several creeks in areas, where the exotic pebbles have been found. For micropaleontological studies, the samples were dried, weighed (most of them weighed 500–750 g) and disintegrated in a solution of sodium carbonate. Then the material was washed through sieves with mesh diameters of 0.63 mm. At least 300 foraminiferal tests were picked from fraction 0.63–1.500 mm, or until all tests were removed from the residue. The foraminiferal slides are housed in the Institute of Geography, Cracow Pedagogical University (Collection No. 09Du).

Petrographic composition of exotics

All of the exotics are fragments of orthogneissic rocks. Polarizing microscope investigations and chemical microprobe analyses of rock-forming minerals revealed the presence of

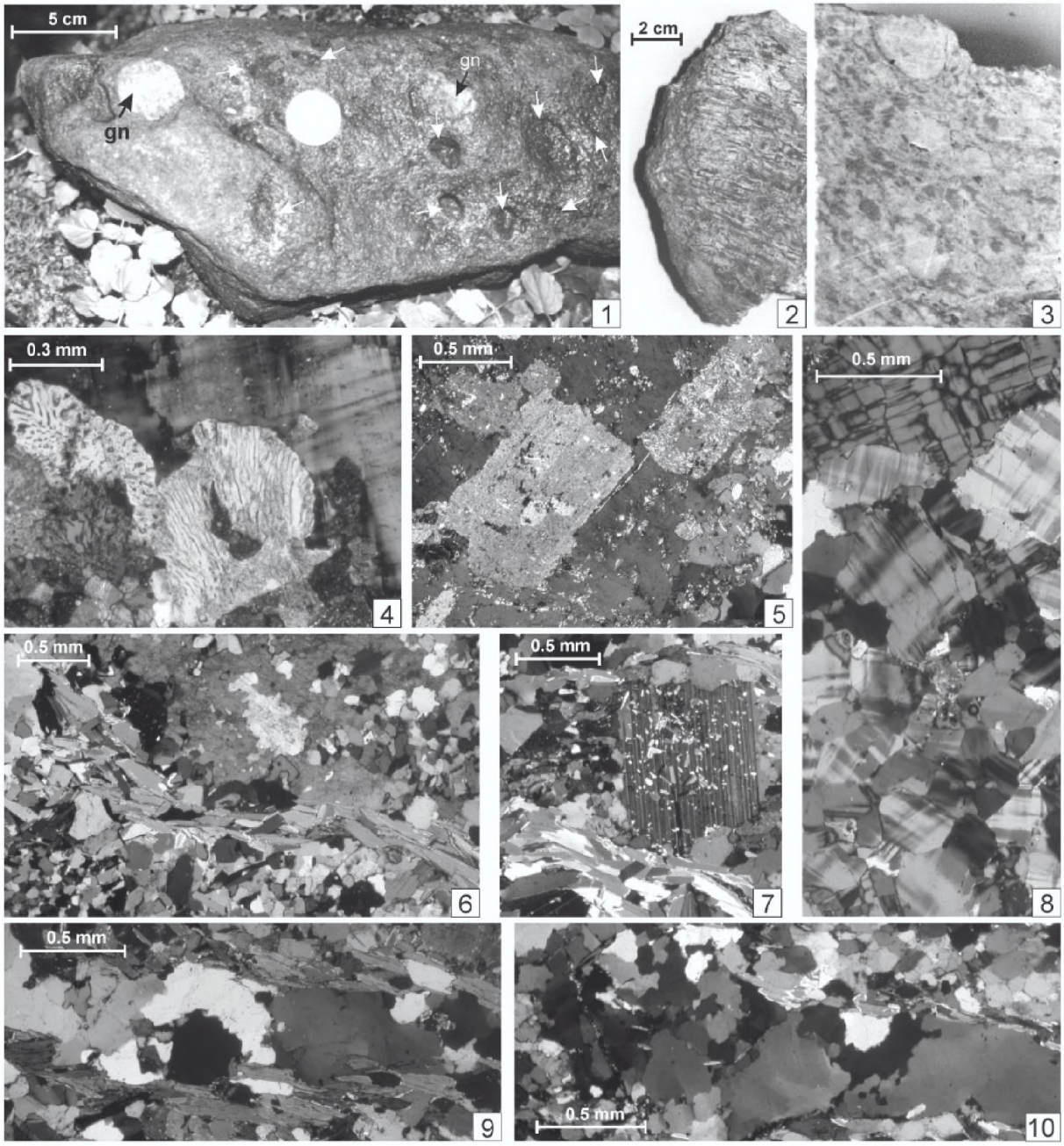

Fig. 3. **1** — Medium- to coarse-grained, non-calcareous sandstone (Cisna Beds) with orthogneiss pebbles (gn); white arrows mark the holes after exotic pebbles; Semenowa stream. **2, 3** — Orthogneiss pebbles from the Cisna Beds: 2 — Połoninka stream; 3 — Kańcz-12/00, polished slab. **4** — Myrmekite intergrowths in marginal part of alkali feldspar augen, Woł-1/99, crossed nicols. **5** — Strongly altered plagioclases (albite or oligoclase) with poorly visible repeated lamellar twinning within alkali feldspar porhpyroblast, Szcz-1/99, crossed nicols. **6** — Porphyroblast composed of chess-board albite (upper part) and asymmetrical fabric of S-C type, Kańcz-12/98, crossed nicols. **7** — Porphyroblast of oligoclase showing repeated lamellar albite twinning and inclusions of light micas in central part, Kańcz-12/98, crossed nicols. **8** — Porphyroblast of small microcline showing typical twinning of cross-hatched or "tartan" type twinning, Woł-13c/99, crossed nicols. **9** — Laminae consisting of pleochroic biotite flakes and crystals of quartz (mosaic and with undulatory extinction), Szcz-1/99, crossed nicols. **10** — Crystals of quartz (mosaic and with undulatory extinction), Kańcz-12/98, crossed nicols.

three types of orthogneisses, differing in colour, structural properties (porphyroblasts sizes, thickness of layers) and mineral composition.

The **first type** represents a medium-grained, medium-banded porphyroblast gneiss showing structural features of foliated granitic-gneiss (samples: Szcz-1/99, Woł-1/99 and Kańcz-11/99). It is greyish in colour, though smaller pebbles are beige coloured with creamy tint. The bands are usually 2–5 mm, sporadically up to 2 cm thick (Fig. 3.2). The grey colouration of bands is due to the presence of biotite. When the biotite is altered, brownish stripes appear and these zones are beige or creamy in colour (s. Woł-1/99). The porphyroblasts are white-

creamy and, in general, 3–8 mm and even up to 1.5 cm in size (Fig. 3.3).

The porphyroblasts consist of alkali feldspars (Or_{93-85} Ab_{7-11}) containing about 1.5 wt. % BaO and showing poorly visible perthite structures. Some alkali feldspars contain plate shaped inclusions of plagioclase — albite (An_{3-9}) (s. Woł-1/99) or oligoclase (An_{12}) (s. Szcz-1/99; Fig. 3.5). These plagioclase crystals are strongly sericitized, displaying a greyish surface and poorly visible repeated lamellar albite twinning. Only one sample (Kańcz-11/99) contains a completely ordered variety of alkali feldspar (microcline), showing repeated lamellar albite and pericline twinning, well-known as typical cross-hatched or "tartan" type twinning.

In all samples, where plagioclase (albite–oligoclase) is in contact with alkali feldspar in marginal parts of porphyroblasts myrmekite form intergrowths (Fig. 3.4) as products of release of silica (quartz) during replacement of potassium feldspar by plagioclases (Hatch et al. 1961). The evolved potassium reacts with alumina and silica to form white mica (phengite), which occurs close to the feldspar porphyroblasts. Deer et al. (1962) attributed the formation of myrmekite to the breakdown of plagioclases during metamorphism. However, its common occurrence in the studied rock is more probably due to strain (cf. Simpson 1985).

The quartz, occurring in the bands is represented by mosaic type crystals and show undulatory extinction between crossed polars. Apart from quartz crystals, bands contain perthitic alkali feldspars Or_{89-90} Ab_{10-8} (consisting of host K-feldspar with irregular albite inclusions of replacement type) and strongly altered plagioclases (andesine-oligoclase An_{30-16}) with repeated lamellar albite twinning. Biotite occurring in bands (Fig. 3.9) is pleochroic, from α pale yellow to γ red brownish (s. Szczaw-1/99) and chloritized to various degrees (ss. Woł-1/99 and Kańcz-11/99). The chemical composition of well-preserved biotite is Fe-rich characterized by atomic ratio Si/Al 2 : 1 and Fe/Mg from 2.87 to 2.34. The MnO content is 0.5 wt. % and TiO_2 from 3.22 to 2.91 wt. %. Phengite is intergrown with biotite and chlorite. The Si/Al ratio in its tetrahedral sites amounts to 3.89–3.66, whilst the Fe/Mg ratio in octahedral sites varies from 1.45 to 2.17. The content of TiO_2 is low, ranging from 0.29 to 0.93 wt. %.

The **second type** is represented by medium-grained, medium-banded orthogneiss containing small porphyroblasts and showing structural features of foliated granitic-gneiss (s. Woł-13c/99). Megascopically, pale creamy quartz-feldspar bands are 3–4 mm thick, whereas quartz bands of similar size are dark grey. White porphyroblasts are up to 5–6 mm in size.

The investigations using optical and electron microscopes have shown that the porphyroblasts consist of large alkali feldspar crystals showing highly ordered structure of microcline type, characterized by typical twinning of cross-hatched or "tartan" type, occurring sectorially in various parts of this mineral. Moreover, these large crystals can be overgrown by fine-blastic microcline. Some porphyroblasts can be "aggregate" in character and consist of small microcline crystals (Fig. 3.8). Microcline ($Or_{91}Ab_9$) contains up to 1.75 wt. % BaO.

Quartz bands are characterized by mosaic crystals and crystals exhibiting undulatory extinction. Apart from quartz, they contain small plagioclase crystals (An_{35} — andesine) showing repeated lamellar twinning. Small white mica flakes occur in their central parts. The process of K-feldspathization of plagioclases is also recorded (irregular, replacement type perthites including K-feldspar). Some alkali feldspar ($Or_{93}Ab_6$) crystals occurring in matrix consist of host K-feldspar. The feldspars contain replacement type inclusions which show the composition of pure albite ($Ab_{97}An_2Or_1$). In the groundmass, small nests occur, filled with fine-blastic microcline, showing characteristic twinning of cross-hatched or "tartan" type. Biotite is usually decolourized and altered into hydrobiotite or completely transformed into iron-rich chlorite (showing Fe/Mg ratio about 2.8). White mica (phengite) occurs close to large microcline augen. The atomic Si/Al ratio in tetrahedral sites amounts to ca. 5.32, whilst the Fe/Mg atomic ratio in octahedral sites varies from 0.9 to 1.00.

The **third type** is represented by strongly cataclastic granitic-gneiss showing properties of partly mylonitized granite (s. Kańcz-12/98). Megascopically, grey bands are 2–5 mm (up to 8 mm) thick, and marked by parallel distribution of white mica. Pale grey porphyroblasts, 3–10 mm in size, are composed of feldspars.

The porphyroblasts consist of chess-board albite (An_8) containing up to 5 wt. % K_2O (Fig. 3.6). The bands consist of quartz with mosaic crystals and crystals with undulatory extinction (Fig. 3.10). There are also crystals of rather well preserved oligoclases (An_{15-17}) showing no zonality, displaying repeated lamellar, albite twinning and containing numerous inclusions of white micas in their central parts (Fig. 3.7). The crystals of host oligoclases contain irregular "spotty" replacement perthites of K-feldspar and quartz veinlets. Asymmetrical fabric of S-C type is observed (Fig. 3.6). Phengite is characterized by atomic Si/Al ratio in tetrahedral sites from 3.87 to 3.67 and atomic Fe/Mg ratio in octahedral sites amounting to 3.05. The content of TiO_2 is constant (1.10–1.15 wt. %) whilst that of MnO does not exceed 0.07 wt. %. Phengite is intergrown with strongly altered biotite (hydrobiotite) and chlorite. This mineral is pleochroic from pale yellow (α) to intense green (γ) and distinctly enriched in iron.

Geochemical characteristics of exotics

Three types of orthogneissic pebbles distinguished on the basis of structural and petrographic investigations were analysed for major, trace and REE elements (Table 1). The first and third distinguished types of orthogneisses (medium-grained orthogneiss, with alkali feldspars porphyroblasts and granitic-gneiss with chess-board albite porphyroblasts, respectively) exhibit similar contents of major elements; only the contents of MgO, CaO and Na_2O display small differences. The second type of orthogneiss (medium-grained orthogneiss with small microcline porphyroblasts) differs from other types by higher content of SiO_2, lower contents of Al_2O_3, TiO_2, Fe_2O_3, MgO and a low Na_2O/K_2O ratio.

The proportions of [(Al+Fe+Ti/3)–K] versus [(Al+Fe+Ti/3)–Na] (after Moine & de La Roche 1968) allowed us to define a kind of protolith of the studied types of gneisses as the orthogneisses (Fig. 4A) — the granite and rhyolite field in the diagram. Another plutonic rock classification diagram ex-

Table 1: Chemical composition of three types of orthogneissic pebbles: **first type** — Szcz-1/99, **second type** — Woł-13c/99, **third type** — Kańcz-12/98. Chromium, molybdenum, tantalum, tin, vanadium, uranium, terbium, wolfram are present below their respective limits (Cr, Ta<1, Sn, Mo, V<5, U, Tb<0.5, W<3).

		Major elements (wt. %)											
Type of orthogneiss	SAMPLE	SiO_2	TiO_2	Al_2O_3	Fe_2O_3	MnO	MgO	CaO	Na_2O	K_2O	P_2O_5	LOI	Total
First type	**Szcz-1/99**	74.10	0.155	14.60	1.56	0.022	0.35	2.01	4.10	1.96	0.07	1.05	99.99
Second type	**Woł-13c/99**	77.17	0.026	13.07	0.39	0.002	0.04	1.10	3.47	3.49	0.03	0.73	99.51
Third type	**Kańcz-12/98**	71.94	0.136	14.91	1.45	0.016	0.53	1.15	4.96	1.51	0.07	1.50	98.17

		Trace elements (ppm)										
Type of orthogneiss	SAMPLE	Ag	Ba	Be	Cd	Co	Cs	Cu	Ga	Hf	Nb	Ni
First type	**Szcz-1/99**	1.4	683	2	0.7	1.0	0.0	4	18	2.5	10	3
Second type	**Woł-13c/99**	2.0	2553	2	0.3	0.0	1.4	9	13	0.7	2	2
Third type	**Kańcz-12/98**	1.3	747	2	0.0	1.0	0.9	4	19	2.3	10	4

		Trace elements (ppm)									
Type of orthogneiss	SAMPLE	Pb	Rb	S (wt. %)	Sc	Sr	Th	U	Y	Zn	Zr
First type	**Szcz-1/99**	14	60	0.000	2.1	468	5.2	0	5	48	106
Second type	**Woł-13c/99**	14	84	0.008	0.2	368	1.4	0	0	15	23
Third type	**Kańcz-12/98**	8	43	0.005	2.4	345	5.3	0.8	4	39	94

		REE (ppm)						
Type of orthogneiss	SAMPLE	La	Ce	Nd	Sm	Eu	Yb	Lu
First type	**Szcz-1/99**	27.3	45	15	2.5	0.7	0.5	0.08
Second type	**Woł-13c/99**	4.8	10	0	0.5	0.5	0.0	0.00
Third type	**Kańcz-12/98**	14.7	27	9	1.8	0.4	0.6	0.08

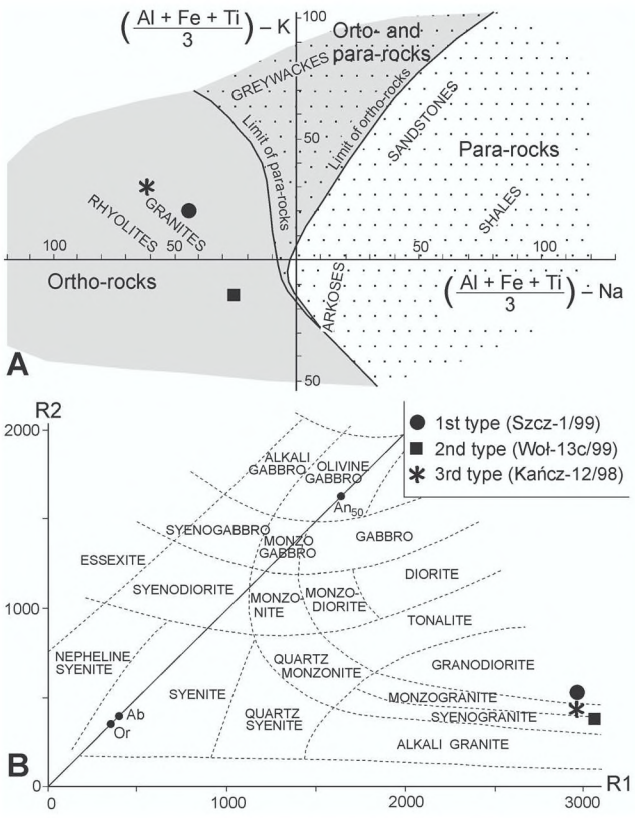

Fig. 4. The position of the granitic protolith on the petrological diagrams for gneissic exotics. **A** — Proportions of [(Al+Fe+Ti/3)-K] vs. [(Al+Fe+Ti/3)-Na]; diagram after Moine & de La Roche (1968). **B** — R1-R2 diagram (after de La Roche et al. 1980): R1 = 4Si-11(Na+K)-2(Fe+Ti), R2 = 6Ca+2Mg+Al (Ab = albite, An_{50} = plagioclase An_{50}, Or = orthoclase).

pressing the balance between *R1* [4Si-11(Na+K)-2(Fe+Ti)] and *R2* [6Ca+2Mg+Al] parameters (de La Roche et al. 1980) shows the position of studied rocks in the fields of granodiorite, monzogranite and syenogranite (Fig. 4B). These geochemical differences of granitoid protolith between the orthogneisses are connected with the above mentioned different amounts of SiO_2, alkalis and Na_2O/K_2O ratio.

Taking into consideration the molar proportions of A/NK and A/CK, the protolith granitoids had a peraluminous character (Maniar & Piccoli 1989; Fig. 5A).

The calculated molar [Al/(Na+K+Ca/2)] parameter, whose values exceed 1.05 for all types of the studied orthogneisses (1.54, 1.24 and 1.37 for the first, second and third type of gneiss, respectively), indicates an S-type granitic protolith (Pitcher 1982). A similar suggestion may be expressed if discrimination indexes, such as prevalence of Na_2O over K_2O (cf. Hovorka & Petrík 1992), low iron content versus SiO_2 (cf. Broska & Uher 2001), low Rb content versus Sr (Fig. 5B), and low Y content versus high SiO_2 content (Fig. 5C) are taken into account. The indexes resemble those, calculated for S-type West-Carpathian granites (Petrík et al. 1994; Broska & Uher 2001), however, their values are transitional to the indexes of I-type granites (Fig. 5B-D). The S-type West-Carpathian granites, the most abundant type in this region, represent peraluminous biotite two-mica granites to granodiorites (for summary of their petrography and chemistry — see Broska & Uher 2001).

Chondrite-normalized trace and REE element data show positive (+) anomalies for Ba, K, Sr, Hf and Y, and negative (-) anomalies for Rb, Nb, Nd, Sm and Ti (Fig. 6). These samples exhibit enrichment in more mobile LIL (large ion lithophile) (Ba, K, Sr) and less mobile HFS (high field strength) (Hf, Y) elements, as well as, impoverishment in LIL (Rb) and HFS

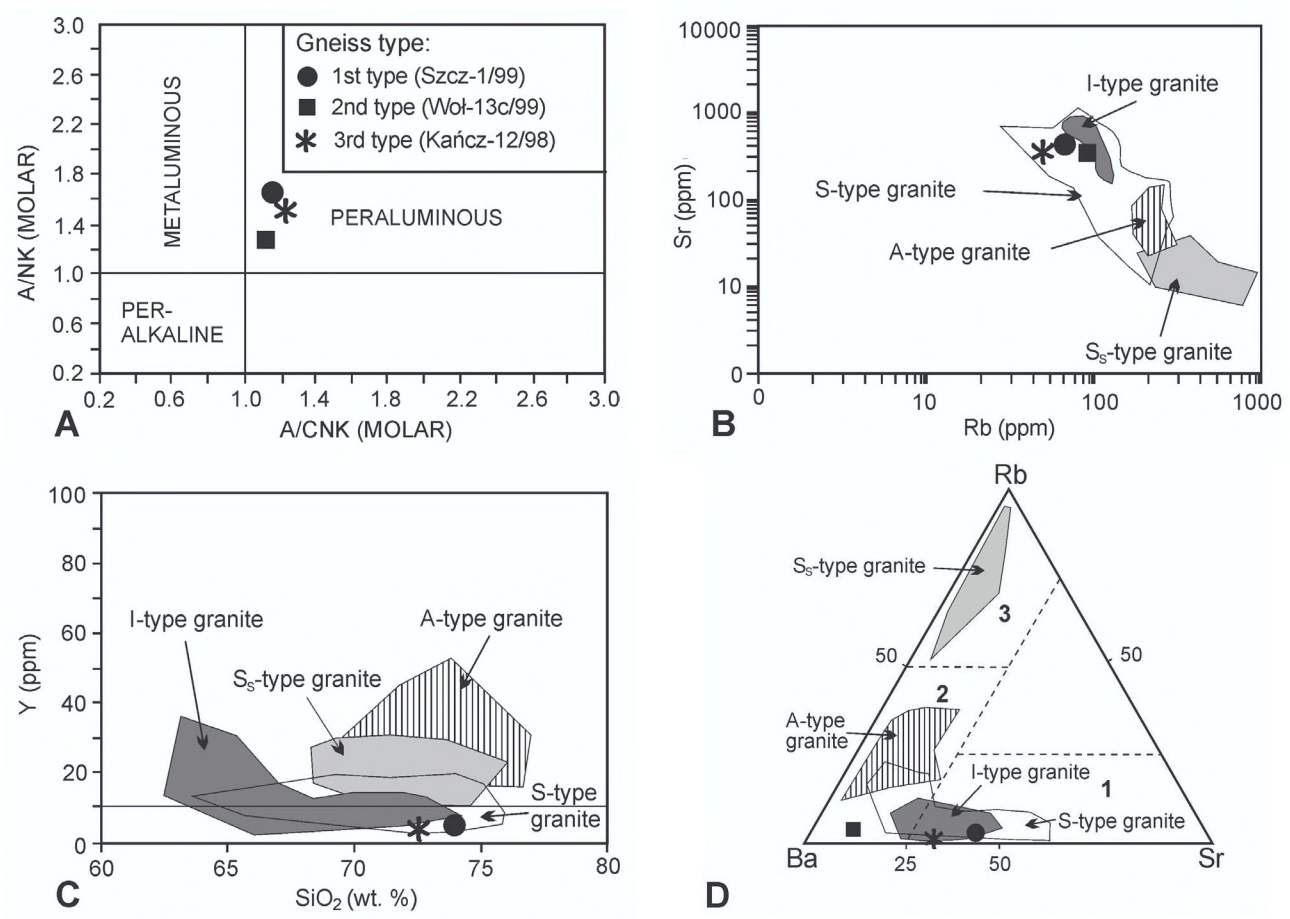

Fig. 5. The position of the granitic protolith for the studied orthogneissic exotics within the discrimination diagrams for granites. **A** — The A/NK (molar) vs. A/CNK (molar) (after Maniar & Piccoli 1989). **B** — Sr vs. Rb plot including data for various types of the Variscan West-Carpathian granitic rocks (after Broska & Uher 2001). **C** — Y vs. SiO_2 plot including data for various types of the Variscan West-Carpathian granitic rocks (after Broska & Uher 2001). **D** — Rb–Ba–Sr ternary discrimination diagram including data for various types of the Variscan West-Carpathian granitic rocks (after Broska & Uher 2001). 1 — poorly evolved granites, 2 — mildly evolved granites, 3 — highly evolved granites.

(Nb, Ti) elements. A little different course of curve for the second type of orthogneiss is observed, when compared with the other two curves. It is expressed in deficiency of Nb, La, Ce, Sm and Ti.

Foraminiferal assemblages in the vicinity of the exotic-bearing layer

Stratigraphic data on the position of the Cisna Beds are known from the western part of the Dukla Nappe within Polish territory. Blaicher (in Ślączka 1971) and Olszewska (1980) determined the age of these deposits on the basis of Foraminifera as the Late Campanian–Early? Paleocene. They suggested a diachronism of their lower boundary. Paleontological data (based also on Foraminifera), obtained by the present author from the Bieszczady Mts have confirmed the suggested age of the Cisna Beds (Bąk 2004). However, the lower boundary could not be precisely determined (Upper Campanian?–Maastrichtian?), because of the lack of taxa diagnostic of age.

Eight samples taken for biostratigraphical study of microfauna from the non-calcareous shales in the lower and middle

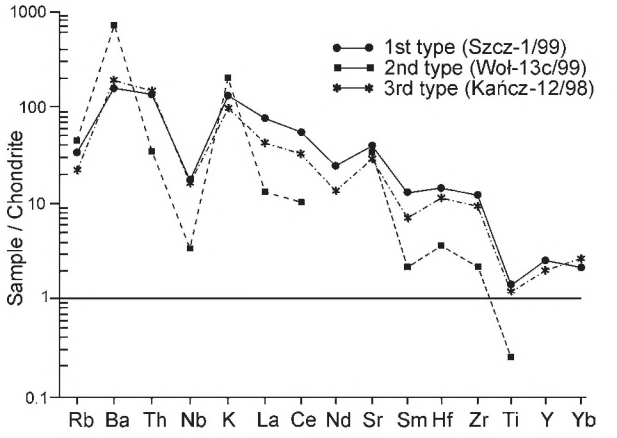

Fig. 6. Chondrite normalized spider diagram (after Tompson 1982) for orthogneissic exotics.

parts of the Cisna Beds include mainly deep-water agglutinated Foraminifera (DWAF) (Fig. 7) and undeterminable radiolarian moulds. The DWAF assemblage is poorly to moderately-diversified (Fisher's alpha index: 3.1–9.1) including

Deep-water agglutinated foraminiferal zones	Pol-3/96	Kańcz-11/99	Kańcz-13/99	Woł-6/96	Woł-11/98	Pol-4/96	Szcz-4/96	Szcz-5/96	Szcz-6/96	Pol-6/96	Szcz-7/96	Woł-7/96
	Łupków B.				Cisna Beds							
	Caudammina gigantea Zone ✱										*R.f.*	
Radiolaria	22	54	11	2			40			2	7	
Ammobaculites sp.	1											
Ammodiscus cretaceus	21			1	1			1		1		11
Ammodiscus glabratus	2							1				
Ammodiscus infimus				1								
Ammodiscus sp.									1			
Annectina grzybowskii									1		1	
Aschemocella grandis	1					1			1			
Aschemocella carpathica										3		
Bathysiphon annulatus		1			1			2	1	1		1
Bathysiphon gerochi					2			2				
Bathysiphon microraphidus				1						1		
Bathysiphon sp.	2	21	9	18	2	12	7	3	5	6	1	6
Caudammina gigantea		3										
Caudammina ovulum	12	3	2	1				1	5	2		2
Conotrochammina whangaia												2
Dorothia indentata				3								
Dorothia trochus									1			
Glomospira charoides	2											1
Glomospira irregularis			1		4		2					2
Glomospira serpens	2				1							
Haplophragmoides porrectus	2				5			1	1			2
Haplophragmoides suborbicularis												2
Haplophragmoides sp.	1				1			1				
Hormosina excelsa	9			5	2							2
Hormosina trinitatensis	1			1								1
Hormosina velascoensis	8			4	4	1		1		1		1
Hyperammina subnodosiformis								3				1
Hyperammina sp.	1	1										
Kalamopsis grzybowskii	16			1	7							
Lituotuba lituiformis	11		1	4								
Nothia sp.					1	5			12			7
Paratrochamminoides irregularis									1			
Paratrochamminoides olszewskii	2											
Paratrochamminoides sp.									1			2
Psammosphaera scruposa	20			3								
Psammosphaera sp.	5		3	2			1	1				2
Recurvoides sp.	9		5	3	23	2	2	13	24	22	3	25
Remesella varians												1
Reophax duplex	7		1	1					1			2
Reophax pilulifer	1											
Reophax sp.	1	1		2		1				1		1
Rhabdammina cylindrica	5		2	3	3	2		2	3	2		4
Rhabdammina sp.	2	25	26	8	12	25	25	7	8	11	1	3
Rhizammina sp.	7			3	4			1				1
Rzehakina epigona				2					1	1		
Rzehakina fissistomata					2						1	
Rzehakina minima									1			
Saccammina grzybowskii	53			4	12	1						2
Saccammina placenta	174			10	13		6	15	22	14	1	26
Spiroplectammina spectabilis												1
Subreophax scalaris	12				3							
Subreophax splendidus									1			
Trochammina sp.	37		1	8	19	3	4	16	22			29
Trochamminoides dubius								1				
Trochamminoides grzybowskii	10			1								
Trochamminoides proteus								1				
Trochamminoides sp.	90		5	10	12		1	4	23	13		30

Fig. 7. Species distribution chart of deep-water agglutinated Foraminifera in the Cisna Beds and Łupków Beds, around the inferred exotic-bearing layer (black star); the Bieszczady Mountains, Poland. ***R.f.*** — *Rzehakina fissistomata* Zone.

siliceous-walled forms with several species of limited stratigraphical significance. The lower part of the Cisna Beds, close to the contact with the Łupków Beds, probably represents the upper part of *Caudammina gigantea* Zone (Maastrichtian? *sensu* Geroch & Nowak 1984), as the occurrences of *R. epigona*, *R. minima* and hormosinids show (Fig. 8.1). First occurrences of *R. varians* (Glaessner) (Fig. 8.3) and *Spiroplectammina spectabilis* (Grzybowski) (Fig. 8.4), which most probably fall within the Middle-Upper Maastrichtian, have not been noted in the sediments from the presented sections. However, they have been found in the lower part of the Cisna Beds, a few kilometers to the north from the studied area (Bąk 2004).

The suggested position of the exotic-bearing layer is close to the position of the micropaleontological sample Szcz-7/96, which was taken from the grey, non-calcareous shales, 10 m above the inferred position of this layer (Fig. 2B). These shales include *Rzehakina fissistomata* (Grzybowski) (Fig. 8.6,7), a Paleocene species (Morgiel & Olszewska 1981; Geroch & Nowak 1984; Olszewska 1997; Bąk, 2004) for which this sample is its first occurrence in this section (Fig. 5). Higher up in the section (s. Woł-7/96; Fig. 2B), other Paleocene species have been found, *Annectina grzybowskii* (Jurkiewicz) (Fig. 8.5) and *Conotrochammina whangaia* Finlay (Fig. 8.8, 8.9), together with a well-diversified DWAF assemblage (Fig. 7).

Discussion

Petrography

The mineralogical composition and structural properties of the granitic protolith was strongly modified. Relics of primary magmatic minerals in orthogneissic pebbles studied are not observed. The rocks studied display structural diversification (S-C fabric), different thickness of quartz, quartz-feldspar, micaceous layers and variable size of porphyroblasts. Microprobe analyses have revealed the differences in the chemical composition of feldspars forming porphyroblasts (alkali- and K-feldspars) and differences in matrix (alkali-, K-feldspars, Na-Ca plagioclases). The effects of metasomatic processes (Na-, K-feldspathization) are observed (replacement perthite) in feldspars, both in porphyroblasts and matrix. Biotite flakes are altered in various degrees (chloritization process). Phengite occurs in micaceous layers and is always overgrown by biotite and chlorite. Phengitic muscovite is stable up to >750 °C and >7 GPa (Catlos & Sorensen 2003). The presence of phengite in the orthogneissic exotics may indicate even the high-pressure metamorphism in terranes of subduction zone slab (Ferraris et al. 2000). However, the recognition of metamorphic facies is here difficult, due to a lack of typical metamorphic mineral assemblages. It is possible that the orthogneisses underwent greenschist facies metamorphism. The orthogneisses from Seward Peninsula, Alaska (Evans & Patrick 1987) are an example of such rocks with similar mineral composition recording such facies conditions.

Geochemistry

The chemical composition of the first and third type of orthogneisses shows that they could originate from the same granitic protolith. The differences in chemical composition of

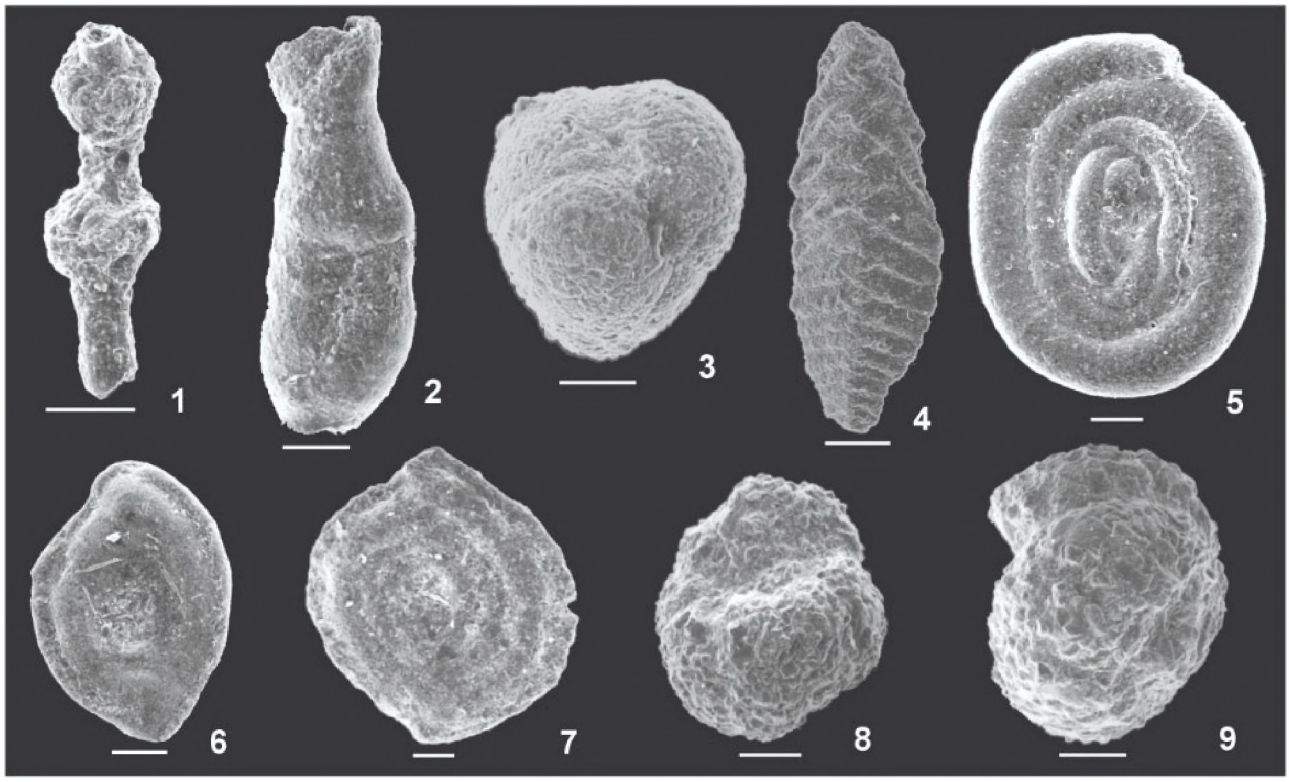

Fig. 8. Paleocene deep-water agglutinated Foraminifera in the vicinity of the exotic-bearing layer, the Dukla Nappe, Polish Outer Carpathians, Bieszczady Mountains: **1** — *Hormosina excelsa* (Dylążanka); Woł-11/98. **2** — *Kalamopsis grzybowskii* (Dylążanka); Woł-11/98. **3** — *Remesella varians* (Glaessner); Woł-7/96. **4** — *Spiroplectammina spectabilis* (Grzybowski); Woł-7/96. **5** — *Annectina grzybowskii* (Jurkiewicz); Szcz-6/96. **6, 7** — *Rzehakina fissistomata* (Grzybowski); Woł-11/98. **8, 9** — *Conotrochammina whangaia* Finlay; Woł-7/96. Scale bar = 100 μm.

the second type of orthogneiss in relation to the two other types could be most probably due to weathering and transport of pebbles from one side, and/or to the effects of earlier processes, which took place in the granitic protolith (e.g. feldspathization and albitization). First of these factors is here probably the most important, because the second type of orthogneiss was recognized from the small pebble (8×5×4 cm), two times smaller than the other studied pebbles. Consequently, it may represent only a fragment of a larger body of banded orthogneisses, which disintegrated during the weathering and transport processes. Thus we can observe only the quartz and quartz-feldspar bands, the most resistant fragments of the original orthogneissic body, and their chemical composition could not be representative for the original rocks. However, on the other hand, the earlier metamorphic processes, such as feldspathization and albitization could be responsible for changes of chemical composition of the original granitic protolith. During recrystallization and formation of orthogneissic structure, under conditions of high-pressure metamorphism, metasomatic processes could operate. Na-metasomatism is suggested on the basis of irregular albite inclusions (replacement perthite type) occurring in the matrix of host K-feldspar crystals (s. Szcz-1/99; Woł-13c/99). These inclusions and additionally, chess-board albite porphyroblasts are also found in other types of orthogneisses (s. Kańcz-12/98). K-metasomatism is related to the observed formation of spotty replacement perthites of K-feldspar in the matrix of host oligoclases (s. Kańcz-12/98).

Geotectonic position of granitic protolith

Various concentrations of trace elements, such as Rb, Y (and its analogue Yb) and Nb (and its analogue Ta) may help in discrimination of granites from different tectonic settings (Pearce et al. 1984). The discrimination diagrams for the studied protolith granitoids, based on Nb–Y, Rb–Y–Nb and Rb–Yb–Ta variations, show that they could represent volcanic-arc or syn-collisional granites (Fig. 9). Other chemical data used for discrimination, such as proportions of Al_2O_3 versus SiO_2 and proportions of (FeO_T+MgO) versus CaO (Maniar & Piccoli 1989) may confirm this suggestion. The studied rocks are classified on such discrimination diagrams as island arc, continental arc or continental collision granitoids (Fig. 10). Taking into consideration their degree of differentiation, they can be classified as poorly-evolved granites *sensu* Broska & Uher (2001; see Fig. 5D).

The partial melting of the crust material during the collisional conditions may also be evidenced on the basis of negative Nb and Ti anomalies, as well as distinct enrichment in Ba, K, Sr, Hf and Y on the chondrite-normalized diagram (Rollinson 1993). However, these data should be discussed carefully, because the same anomalies may be an effect of hydrothermal

or metasomatic activity in the protolith of granitic rocks and of later metamorphic processes (e.g. albitization resulted in Nb negative anomaly; Rollinson 1993).

So, in conclusion, the presented petrographical and geochemical data, related to typology of protolith granites and their geotectonic setting, represent features, typical of the peraluminous, poorly-evolved, S-type granites, widely known from the Western Carpathians (see summary in Cambel et al. 1985; Broska & Uher 1991; Uher & Gregor 1992; Uher et al. 1994; Petrík & Broska 1994; Petrík et al. 1994; Broska & Uher 2001). According to their mineralogical and geochemical characteristics, Broska & Uher (2001) suggested that this type of granite group exhibits features of orogen-related crustal granites, connected with collisional and extensional regime during and after collision with various contribution from the mantle especially in the post-collisional tectonics. They were formed in the Western Carpathians during the meso-Variscan, Early Carboniferous period (with culmination at about 350 Ma; Cambel et al. 1990).

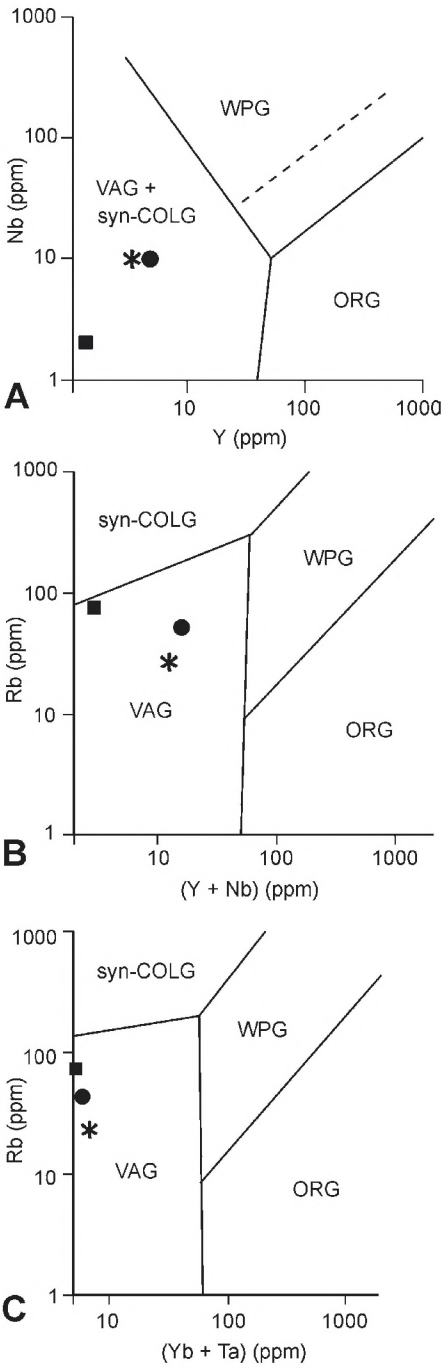

Fig. 9. **A** — Nb vs. Y diagram (after Pearce et al. 1984). **B** — Rb vs. (Y+Nb) diagram (after Pearce et al. 1984). **C** — Rb vs. (Yb+Ta) diagram (after Pearce et al. 1984). **syn-COLG** — syn-collisional granites, **WPG** — within-plate granites, **VAG** — volcanic-arc granites, **ORG** — ocean-ridge granites. For explanations of gneiss symbols — see Fig. 5.

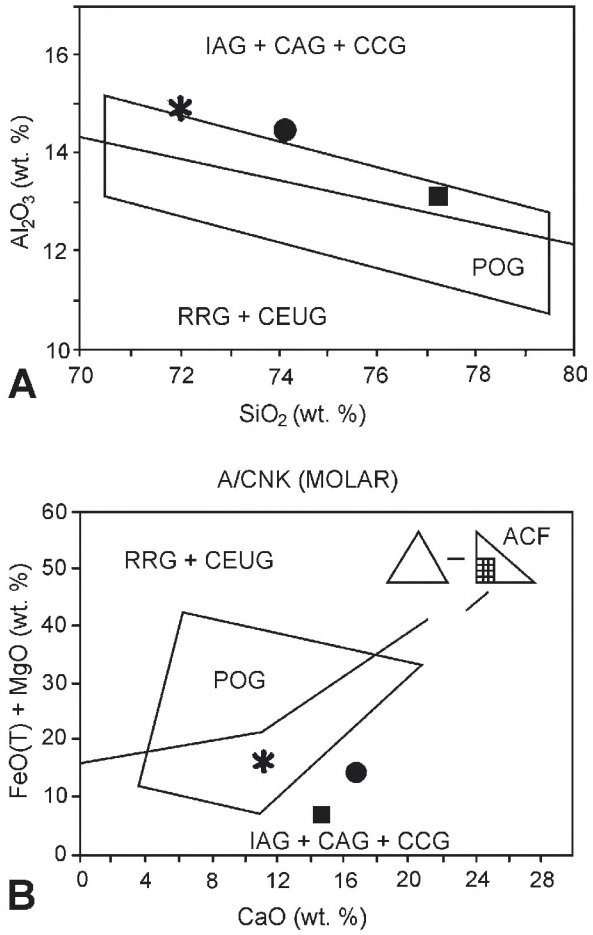

Fig. 10. **A** — Al_2O_3 vs. SiO_2 diagram (after Maniar & Piccoli 1989). **B** — (FeO_T+MgO) vs. CaO diagram (after Maniar & Piccoli 1989). **IAG** — island-arc granitoids, **CAG** — continental-arc granitoids, **CCG** — continental collision granitoids, **POG** — post-orogenic granitoids. For explanations of orthogneiss symbols — see Fig. 5.

Age of orthogneissic exotics

Recently, isotope study of orthogneissic-exotic pebble (Szcz-1c/99) has been carried out on separated mineral phase using the K/Ar method. The age of white micas from this peb-

ble, representing the first type of orthogneiss was calculated as 304.9 ± 11.4 Ma (for details — see Poprawa et al. 2004). The obtained Late Carboniferous date, which represents a metamorphic event in the rocks, may suggest that the protolith granites may have intruded earlier, during the main Variscan magmatism event in the Carpathians, around 350–340 Ma (Burchart et al. 1987; Cambel et al. 1990; Petrík et al. 1994; Petrík & Kohút 1997; Petrík 2000; Poller et al. 2000; Putiš et al. 2003).

Stratigraphic position of exotic-bearing layer

The biostratigraphy of the Middle–Upper Campanian, Maastrichtian and Paleocene of deep-water sediments in the Carpathians renders some problems. Planktonic species, usually poorly preserved, occur as single redeposited specimens, or they are absent. On the other hand, abundant deep-water agglutinated Foraminifera (DWAF), which are in many cases the only microfossils in the sediments, include long-ranging forms. Practically, all of them may occur in both the uppermost Cretaceous and Paleocene sediments. Only two long-ranging taxa may be used to distinguish the Upper Cretaceous from Paleogene sediments: *Caudammina gigantea* (Geroch) — typical of the Campanian–Maastrichtian (Geroch & Nowak 1984) and *Rzehakina fissistomata* (Grzybowski), which occurs over the whole Paleocene section. Unfortunately, both taxa are found as single specimens, being especially rare near their last appearance data (e.g. *C. gigantea* is extremely rare in the Upper Maastrichtian). Several DWAF taxa appeared progressively during Campanian–Maastrichtian times. It concerns such species as *Hormosina excelsa* (Dylążanka), *Hormosina velascoensis* (Cushman), *Rzehakina minima* Cushman et Renz, which have FADs in the Campanian, and *Rzehakina epigona* (Rzehak), *Remesella varians* (Glaessner), *Glomospira diffundens* (Cushman et Renz) and *Spiroplectammina spectabilis* (Grzybowski) which appear progressively in the Maastrichtian. However, a precise correlation of their FADs is not established yet (for details — see Bąk 2000, 2004).

Such progressive appearance of these DWAF species took place within the lower part of the Cisna Beds, below the exotic-bearing layer. This shows at least the Maastrichtian age of this part of the Cisna Beds.

The paleontological data, obtained from the shales, near to the inferred position of the exotic-bearing layer, and from the overlying sediments show that this layer was laid down close to the Cretaceous/Tertiary (K/T) boundary, most probably during the earliest Paleocene, as indicated by the first appearance of *R. fissistomata*, noted in the Carpathians just above the K/T boundary (Bubík et al. 1999).

Source rocks of the exotic-bearing layer and the Cisna Beds

In order to identify the provenance of the studied pebbles, and also to evaluate the possibility that the orthogneissic rocks were the source rocks for the siliciclastic material of the flysch series of the Cisna Beds, the analytical data from the pebbles have been compared with the petrographic composition of the Cisna-type sandstones. This comparison is based on our studies in various localities of the Bieszczady Mountains (Fig. 11; Table 2), and on additional petrographic data, related to occurrences of the Cisna Beds in both the Polish (Ślączka 1971) and Slovak parts (Koráb & Ďurkovič 1978) of the Dukla Nappe.

Table 2: Petrographic composition of the fine-grained conglomerate of the Cisna Beds, Bieszczady Mountains, Poland. Total content calculated as 100 %.

	Quartz					Feldspars				Other minerals										Rock fragments									
Samples	Mosaic crystal	Crystal with undulatory extinction	Crystal with normal extinction	Corroded crystal	Myrmekite	Plagioclase with repeated lamellar twinning	Microcline	Pertite-orthoclase	Strongly altered feldspar	Biotite	Calcite	Chlorite	Muscovite	Glauconite	Ferrous oxides and hydrooxides	Tourmaline	Rutile	Zircon	Garnets	Gneisses and granitic-gneiss	Crystalline schists	Crystalline garnet-bearing schists	Phyllites	Siliceous rocks	Clayey shales	Siderites?	Volcanic rocks	Sandstones and mudstones	Cement
Kańcz-11/99	38.4	12.1	6.3	0.5		2.4	4.8	5.1	3.4					0.5	0.5					2.7	1.7		1.2	0.2					20.2
Semen-lewy-17/1/99	36.2	13.1	7.9		0.1	3.6	0.7	2.4	7.0	0.1			0.3	0.3	1.5	0.1	0.1			1.4	1.8		3.1	0.4			0.1		19.8
Szyp-wierzch-4/1/98	34.3	9.3	6.3	1.1	0.2	2.3	0.8	4.9	11.5	0.5	1.1		1.1	0.2	1.1					2.9	2.5		1.0	0.5		0.2		0.3	17.9
Chresty-1/99	36.5	6.8	3.5	0.6		2.2		4.0	5.5	0.8			0.8		1.2					10.5	8.1		3.3	1.4		0.7	1.3	2.4	10.4
Wlk. Semen-2/99/a	18.0	2.6	1.6			0.2	0.3	6.3	1.0	0.1			0.1		2.0					51.3	5.2		0.4	0.7	1.6	1.1		0.7	6.8
Wol-13b/98	28.9	10.0	9.1	1.0		2.3	1.2	8.8	5.5	1.0		0.2	0.7	0.6	2.9					9.2	8.2		0.1	0.5					9.8
Wołosate-3/98/c	26.9	7.7	7.6			0.2			3.5	1.0		0.1	2.3	0.1	3.7	0.1		0.1	0.4	16.3	16.1	0.1	3.5	0.6			0.1		9.6

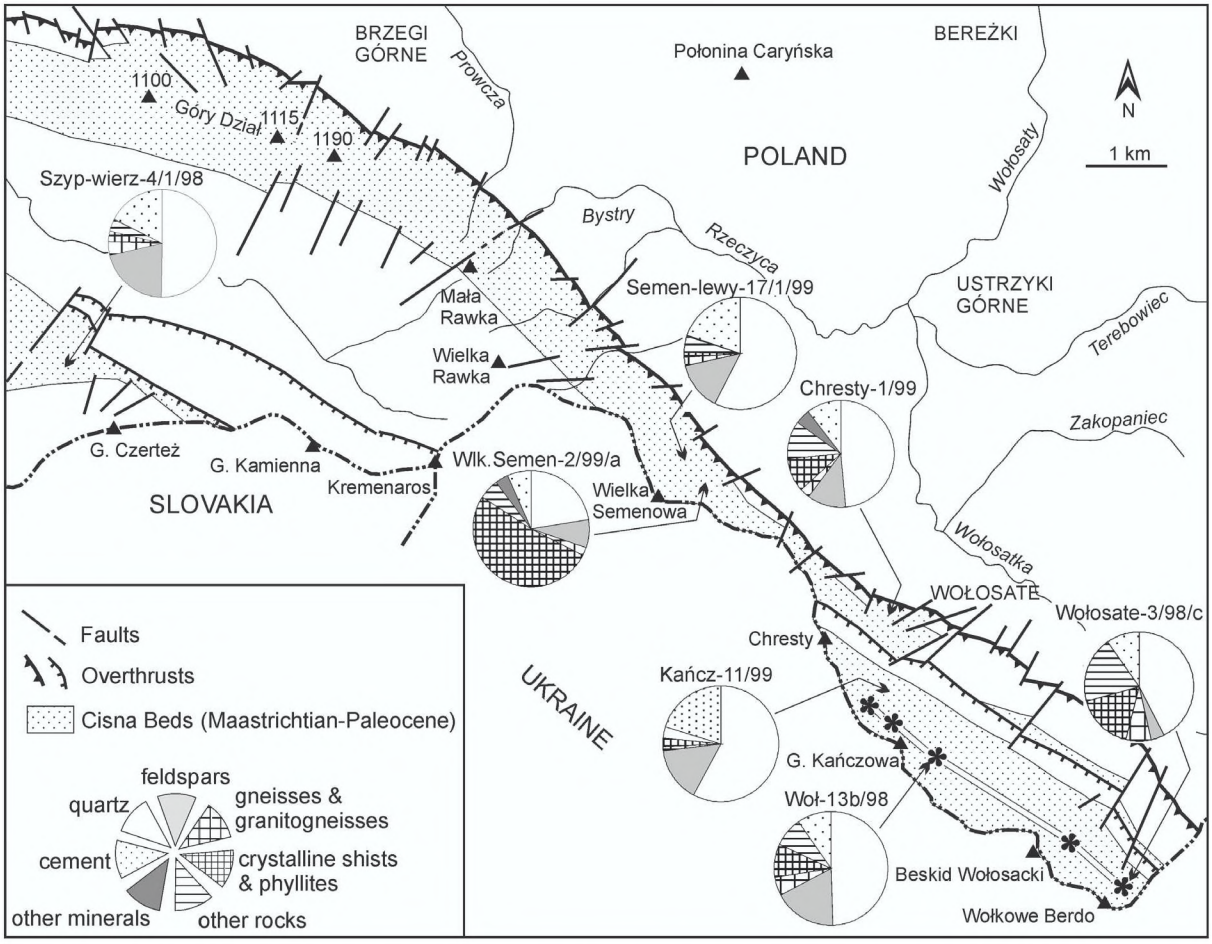

Fig. 11. Petrographic composition of the Cisna-type sandstones from the studied area; northern part of the Dukla Nappe, Bieszczady Mountains, Poland.

Structural features, textural features and mineralogy of the Cisna-type sandstones

Detrital grains in the sandstones vary in the degree of rounding. According to Pettijohn's (1975) classification, they are subrounded, rounded and well rounded. Their contacts are straight-line, but convex-concave are also observed. The size of grains is diversified, mineral grains range from 0.2 to 2.1 mm, whereas rock fragments — from 0.9 to 2.5 mm. In some samples, the sandy grain size is accompanied by gravelly grain size, represented by mineral and rock fragments, 3.5–7.0 mm in size. In the sample Wlk. Semen-2/99/a, the size of detrital grains and rock fragments exceeds 2.0 mm and the volume of gravelly grain size is higher than 50 %.

Quartz is dominant among detrital minerals, forming commonly mosaic crystals and crystals exhibiting undulatory extinction (Fig. 12.8). The present study has confirmed Ślączka's opinion (1971) that the majority of detrital feldspar grains are strongly altered. Their content is significant and amounts to 11.6 vol. %, whilst that of unaltered feldspars, represented mainly by orthoclase perthite (Fig. 12.3) and less common microcline (Fig. 12.7), showing typical-twinning cross-hatched or "tartan" type and repeated lamellar-twinning plagioclases (Fig. 12.6) is distinctly lower. The fragments of myrmekite (Fig. 12.5) and phyllosilicates occur in subordinate amounts, while white mica is more common than biotite. Biotite is more easily altered, showing different stages of chloritization. Small chlorite flakes and glauconite aggregates are also observed. Opaque minerals are represented mainly by anhydrous and hydrated iron oxides.

The sandstones also contain heavy minerals, including garnets, zircon, tourmaline and rutile (Table 2). The amount of garnets is the highest. Though these minerals are not resistant to chemical weathering, they are well preserved during transport and mechanical disintegration. This conclusion is consistent with the data reported by other authors (Ślączka 1971; Koráb & Ďurkovič 1978; Winkler & Ślączka 1992, 1994) for heavy minerals of the Cisna Beds. All these authors described the population dominated by garnet and very stable minerals (zircon, tourmaline and rutile) (up to 95 % in frequency), with accessory of brookite, anatase, titanite, apatite and epidote.

Rock-fragment grains are the other significant component of the Cisna-type sandstones. They are represented by crystalline rocks (Fig. 11, Table 2) showing medium degree of regional metamorphism — mainly orthogneisses and schists (in s. Woł-13b/98 — also garnet-bearing schist). The content of crystalline rocks is variable. It is the highest in sandstones containing gravelly grain size (18.6–32.4 vol. %) and in con-

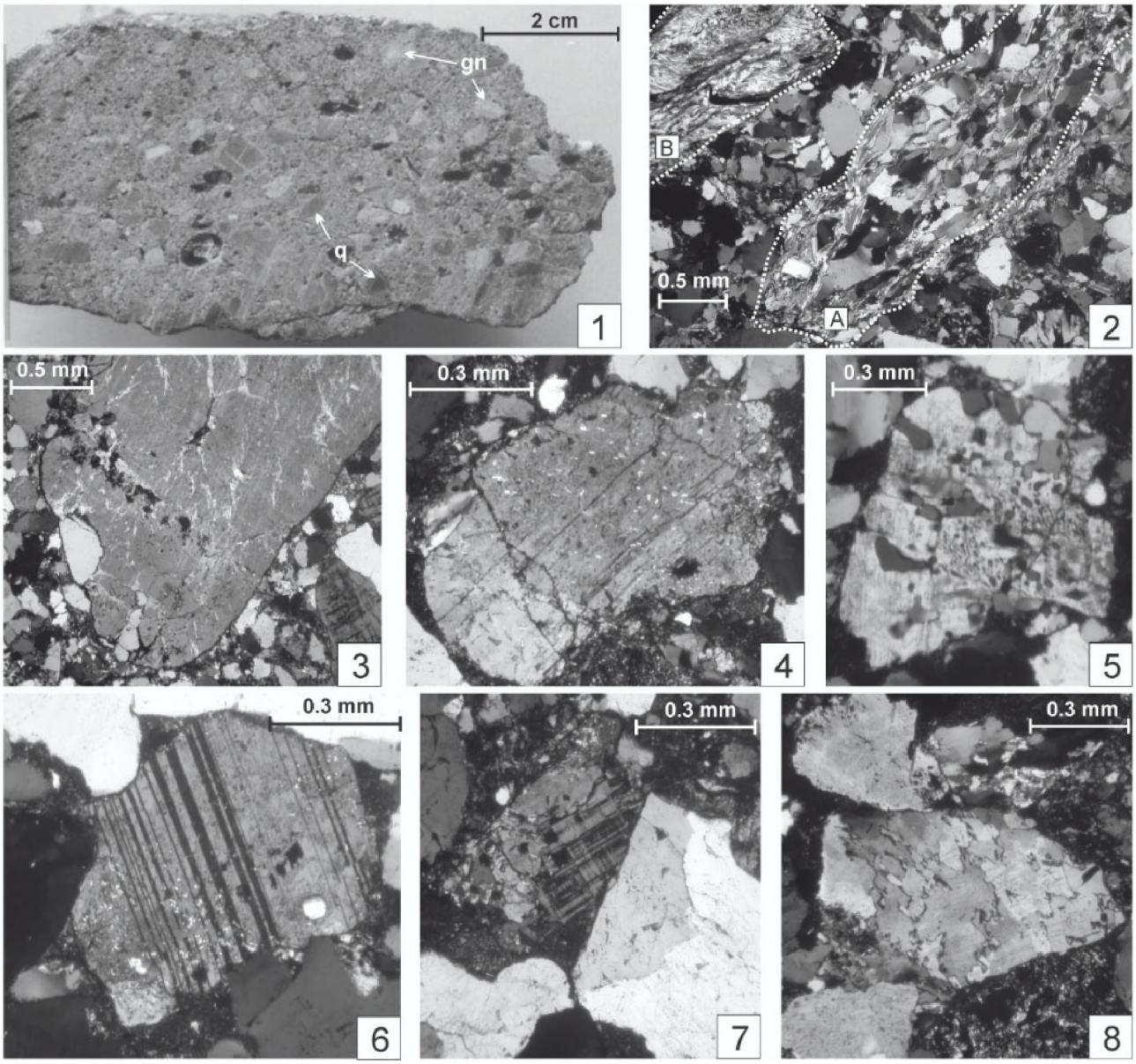

Fig. 12. **1** — Gravelstone of the Cisna Beds with abundant white pebbles of orthogneiss fragments (**gn**) and dark grey quartz (**q**), Woł-3/98, polished slab. **2–8** — Micrographs of grains from sandstones of the Cisna Beds which derive from decomposition of orthogneisses: 2 — Crystalline rocks fragments; **A** — orthogneiss grain, **B** — phyllite grain, Wołosate-3/98/c, crossed nicols. 3 — Grain of perthitic orthoclase, Woł-13b/98, crossed nicols. 4 — Plagioclase grain, Kańcz-11/99, crossed nicols. 5 — Fragment of myrmekite, Semen-lewy-17/1/99, crossed nicols. 6 — Plagioclase grain showing repeated lamellar albite twinning, Semen-lewy-17/1/99, crossed nicols. 7 — Fragment of orthogneiss (microcline and mosaic quartz crystalloblasts), Kańcz-11/99, crossed nicols. 8 — Mosaic quartz grain, Semen-lewy-17/1/99, crossed nicols.

glomerates (s. Wlk. Semen-2/99/a: 56.8 vol. %). Fragments of phyllites and siliceous, ferruginous, clayey and effusive (volcanic) rocks are less common. Some thick-bedded layers (not studied here) may also contain sedimentary clasts (mainly non-calcareous shales).

The Cisna-type sandstones contain predominantly contact-porous and basal cement. In some samples, matrix-type cement also occurs, where the main detrital quartz and less common feldspars are much smaller in size. The content of cement is diversified, as documented by planimetric analyses (Table 2). In sandstones lacking the gravelly grains (pebbles), it varies from 10 to 20 vol. % and does not exceed 10 vol. % in sandstones containing some admixture of gravelly material. In conglomerates, the content of cement is distinctly low (ca. 6.8 vol. %). The majority of clastic rocks contain clayey-ferruginous cement, but locally it is calcareous, corroding detrital feldspar grains. This phenomenon may be related to the presence of secretional forms — calcite veinlets and nests.

In the classification F-Q-R and M-Q-F+R diagrams (for details, see Fig. 13A,B) showing the petrographical and struc-

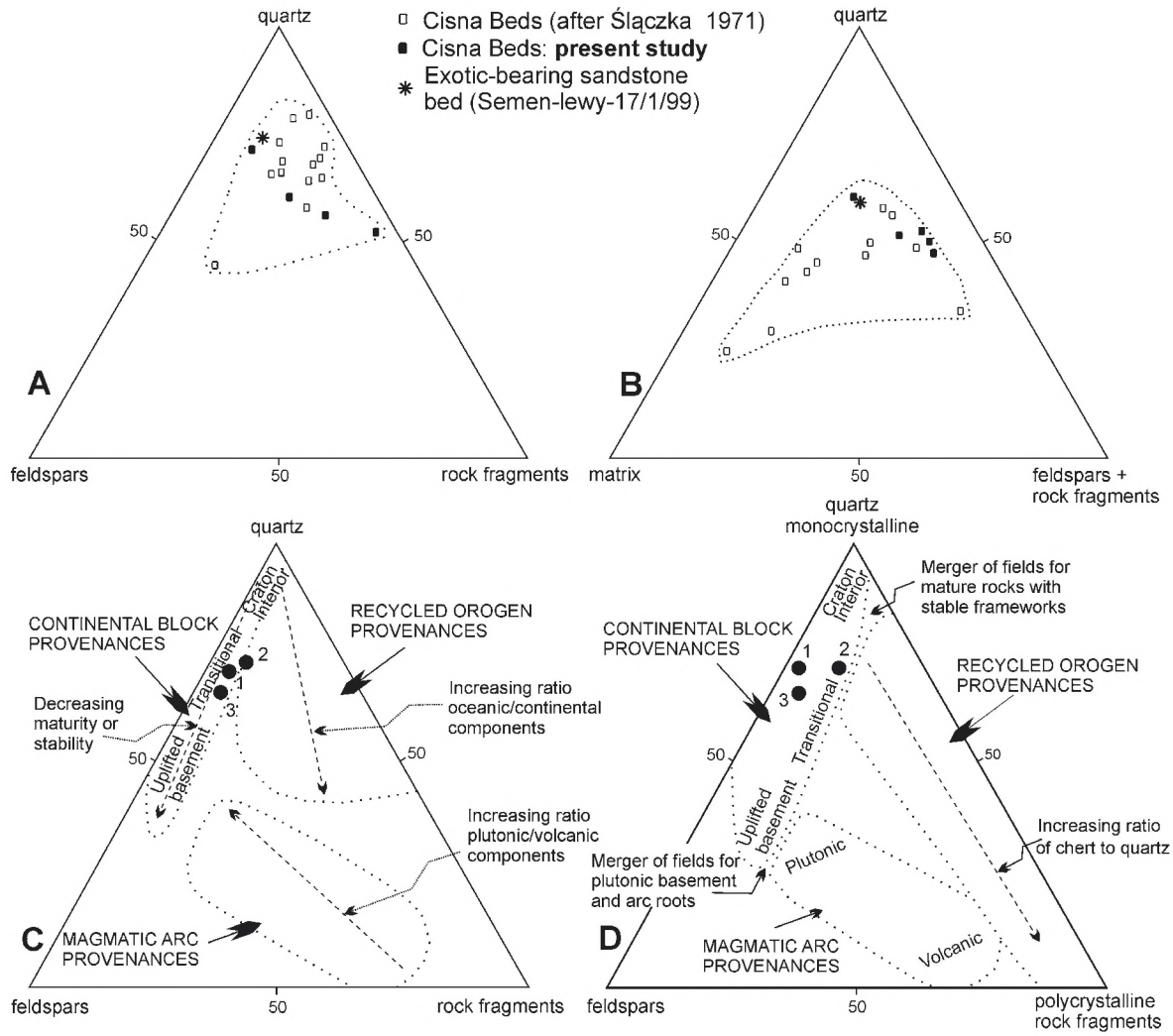

Fig. 13. A, B — Mineral-petrographic composition of sandstones in the Dukla Beds including data from literature (Ślączka 1971; Koráb & Ďurkovič 1978): A — Content of quartz, feldspars and rock fragments calculated as 100 %. B — Content of quartz, feldspars together with rock fragments and matrix calculated as 100 %. **C, D** — Ternary discrimination diagrams of the coarse-grained sandstones of the Cisna Beds, related to different tectonic provenances (after Dickinson & Suczek 1979). 1 — Kańcz-11/99, 2 — Semen-lewy-17/1/99, 3 — Szyp-wierz-4/1/98.

tural features, the Cisna-type sandstones containing pebbles of orthogneissic rocks are plotting in similar fields to those of sandstones examined by Ślączka (1971) from the western part of the Dukla Nappe.

In the F-Q-L and F-Q_m-L_t diagrams showing the provenances of material (Dickinson & Suczek 1979), the studied Cisna-type sandstones are plotted in the field of continental block provenances (Fig. 13C,D).

Cisna-type sandstones versus orthogneissic exotics

Detailed petrographic studies of sandstones and conglomerates from the series containing orthogneissic pebbles have confirmed that the continental crust rocks consisting of orthogneisses and granitic-gneisses were the source material for the Cisna-type sandstones.

The following data indicate that orthogneisses were the dominant rocks of the source area for the Cisna-type sandstones: **1** — prevalence of clasts of mosaic quartz (up to 39 vol. %), **2** — considerable content of crystals of quartz exhibiting undulatory extinction, **3** — myrmekite fragments, **4** — microcline clasts showing typical twinning cross-hatched or "tartan" type, **5** — alkali feldspar clasts displaying perthite structures, **6** — plagioclase clasts containing light mica inclusions in central parts, **7** — occurrence of flakes of white mica and sporadically strongly altered flakes of biotite (hydrobiotite), **8** — occurrence of small fragments of gneisses (quartz + feldspars, quartz + plagioclase, quartz + K-feldspar + plagioclase, K-feldspar + plagioclase) and larger fragments of orthogneisses in gravelly grain size in sandstone and conglomerate samples.

The occurrence of granitic rocks as the source rocks of the Cisna-type sandstones is here documented by various mineral assemblages, found in the studied samples. They include quartz + feldspars (alkali feldspar + K-feldspar + plagioclases) + white mica (phengite) + biotite (chlorite).

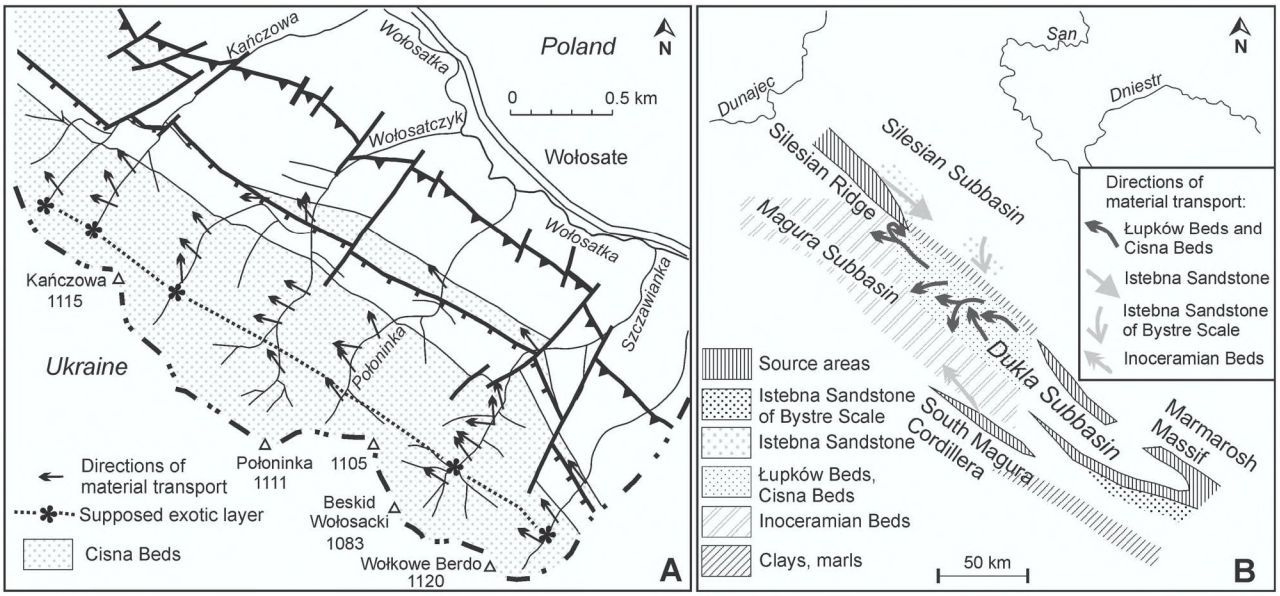

Fig. 14. **A** — Directions of paleotransport in the Cisna Beds near the inferred exotic-bearing layer; Wołosatka drainge basin, Bieszczady Mountains, Poland. **B** — Directions of material transport in the Łupków and Cisna Beds (Campanian–Paleocene) and position of the source area (after Książkiewicz 1962; Ślączka 1971; supplemented).

Provenance of orthogneissic exotics

The exposures with exotics in the Dukla Nappe do not provide direct information about the location of the source area for the orthogneissic exotics. Petrographic affinities between orthogneissic pebbles and mineral/rock fragments grains of the Cisna-type sandstones unequivocally show on the same provenance of them. Thus we suggest that these deposits were transported from south-east, like the material of the Cisna-type sandstones. The directions of material transport, measured from hieroglyphs in the studied area are fairly stable, from 100° to 160° (Fig. 14A). Comparison of the petrographic composition of the Dukla-type sandstones, textural features of the sandstones (e.g. ratio of grains versus matrix) and contents of coarse-grain material between the western and eastern parts of the Dukla Nappe (Ślączka 1971; Koráb & Ďurkovič 1978) are additional factors which point to the location of the source area south-east of the studied area.

The paleogeography of the Dukla Basin during the Senonian and Paleocene was presented by Książkiewicz (1962), Ślączka (1971), Danysh (1973) and Koráb & Ďurkovič (1978). According to these authors, the turbidites of the Cisna Beds were derived from a cordillera, located to the SE (Fig. 14B). Sedimentological and petrographical data, presented by Ślączka (1959) from the Bystre Scale (Upper Cretaceous-Paleocene Istebna Beds of the Silesian Basin) show that the Dukla Basin was restricted to the north by the south-eastern extension of the Silesian cordillera. On the other hand, Danysh (1973) suggested an occurrence of the so-called "Central Cordillera" within the south-eastern part of the Dukla Basin. It was the source area for thick-bedded, coarse-grained turbidites of the Upper Berezny Beds (equivalent of the Cisna Beds in Ukrainian territory). Most probably, an extension of this cordillera, which is recently regarded as the NE part of the Marmarosh massif (Hamor et al. 1989; Poprawa et al. 2002) could be the source area of the Cisna Beds in the Polish part of the Dukla Basin. The foraminiferal assemblages (*Saccammina-Bathysiphon* biofacies; Bąk 2004) show on deep-water sedimentation, below the calcium compensation depth during the Maastrichtian–Paleocene in the Dukla Basin. According to Ślączka (1971) and Leško et al. (1960), the thickness distribution of the Cisna Beds, which gradually disappear in the more inner folds of the Dukla Nappe, show that the axis of maximum deposition was near the northern margin of the Dukla Basin.

Conclusions

1 — The layer with exotics may be a useful correlation horizon on a regional scale in the Campanian–Paleocene monotonous flysch series of the Dukla Nappe. The exotics from the Dukla Nappe probably occur in a layer, which extends over a distance of at least 3 km. This layer occurs in the southern limb of the northernmost anticline of the Dukla Nappe, within the thick series of thick-bedded and coarse-grained sandstones of the Cisna Beds, 550 m above their lower boundary.

2 — The exotic pebbles include three types of granite derived orthogneisses: 1 — medium-banded orthogneiss with alkali feldspar porphyroblasts showing structural features of foliated granitic-gneiss, 2 — medium-banded orthogneiss containing small microcline porphyroblasts and showing structural features of foliated granitic-gneiss, and 3 — strongly cataclastic granitic-gneiss with chess-board albite porphyroblasts showing properties of partly mylonitized granite. The petrographic composition of the orthogneisses shows that the protolith of the orthogneisses points to granites metamorphosed under conditions of greenschist facies.

3 — The chemical composition of the exotic pebbles confirms that they represent orthogneisses, which point to peraluminous, poorly-evolved, S-type granites, widely known from the Variscan crystalline basement of the Western Carpathians. According to their mineralogical and geochemical characteristics, they exhibit features of orogen-related crustal granites. The discrimination diagrams, based upon major elements and trace elements show that the protolith rocks could represent active continental margin or continental collision (syn-collisional) granites.

4 — The Late Carboniferous age date of white micas from the orthogneissic pebble (first type of orthogneiss; K/Ar method: 304.9±11.4 Ma; Poprawa et al. 2004) is related to the metamorphism event of the rocks. It may suggest that the protolith granites may have intruded during the main Variscan magmatism event in the Carpathians, coinciding with interval 350–340 Ma.

5 — The biostratigraphical data on deep-water agglutinated Foraminifera suggest the position of the exotic-bearing layer in the lowermost Paleocene, close to the K/T boundary.

6 — Petrographic affinities between orthogneissic pebbles and mineral/rock fragments grains of the Cisna-type sandstones show the same provenance for them. These deposits were transported from the northeast extension of the Marmarosh massif. During the Maastrichtian and Paleocene, the massif had the character of continental source bearing cordillera, formed mainly of orthogneissic and granitic rocks.

Acknowledgments: Thanks are due to Prof. G. Haczewski (Cracow Pedagogical University) for his discussion during the mapping of the study area and for improving the English text of the manuscript, and Prof. W. Narębski (Museum of the Earth, Polish Academy of Sciences, Warsaw) for critical reading of the geochemical part of this paper. Thanks are extended to the Directors of the Bieszczady National Park for the permission to carry out the fieldwork. The authors are indebted to Jadwiga Faber M.Sc. (Scanning Microscope Laboratory of the Institute of Zoology, Jagiellonian University) for scanning electron micrographs and chemical microprobe analyses. Many thanks are also due reviewers of the manuscript: Prof. N. Oszczypko, Dr. L. Švábenická, Dr. O. Krejčí, Dr. I. Petrík and two anonymous persons for constructive comments.

References

Bąk K. 2000: Biostratigraphy of deep-water agglutinated Foraminifera in Scaglia Rossa-type deposits of the Pieniny Klippen Belt, Carpathians, Poland. In: Hart M.B., Kaminski M.A. & Smart C. (Eds.): Proceedings of the Fifth International Workshop on Agglutinated Foraminifera, Plymouth, England, September 12–19. 1997. *Grzybowski Found. Spec. Publ.* 7, 15–40.

Bąk K. 2004: Upper Cretaceous-Palaeogene foraminiferal biofacies in the deep-water flysch environment; a case study from the Eastern Carpathians. In: Kaminski M.A. & Bubík M. (Eds.): Proceedings of the Sixth International Workshop on Agglutinated Foraminifera. *Grzybowski Found. Spec. Publ.* 8, 1–56.

Broska I. & Uher P. 1991: Regional typology of zircon and their relationships to allanite-monazite antagonism (on example of Hercynian granitoids of the Western Carpathians). *Geol. Carpathica* 42, 271–277.

Broska I. & Uher P. 2001: Whole-rock chemistry and genetic typology of the West-Carpathian Variscan granites. *Geol. Carpathica* 52, 79–90.

Bubík M., Bąk M. & Švábenická L. 1999: Biostratigraphy of the Maastrichtian to Paleocene distal flysch sediments of the Rača Unit in the Uzgruň section (Magura group of nappes, Czech Republic). *Geol. Carpathica* 50, 33–48.

Burchart J., Cambel B. & Král' J. 1987: Isochron reassessment of K-Ar dating from the West Carpathian crystalline complex. *Geol. Zbor. Geol. Carpath.* 41, 131–170.

Cambel C., Petrík I. & Vilinovič V. 1985: Variscan granitoids of the Western Carpathians in the light of geochemical-petrochemical study. *Geol. Zbor. Geol. Carpath.* 36, 204–218.

Cambel C., Král' J. & Burchart J. 1990: Isotopic geochronology of the West Carpathian crystalline complex with catalogue of data. *Veda*, Bratislava, 1–183 (in Slovak with English summary).

Catlos E.J. & Sorensen S.S. 2003: Phengite-based chronology of K- and Ba-rich fluid flow in two paleosubduction zone. *Science* 299, 92–95.

Danysh W.W. 1973: Geology of the western part of the Ukrainian Carpathians. *Naukova dumka*, Kijev, 1–116 (in Russian).

Deer W.A., Howie R.A. & Zussman J. 1962: Rock-forming minerals; part 5. *Longmans, Green and Co Ltd.*, London, 1–435.

de La Roche H., Leterrier J., Grande Claude P. & Marchal M. 1980: A classification of volcanic and plutonic rocks using R1-R2 diagrams and major element analyses — its relationships and current nomenclature. *Chem. Geol.* 29, 183–210.

Dickinson W.R. & Suczek C.A. 1979: Plate tectonics and sandstone compositions. *Bull. Amer. Assoc. Petrol. Geol.* 63, 2164–2182.

Evans B.W. & Patrick B.E. 1987: Phengite (3T) in high-pressure metamorphosed granitic orthogneisses, Seward Peninsula, Alaska. *Canad. Mineralogist* 25, 141–158.

Ferraris C., Chopin C. & Wessicken R. 2000: Nano- to micro-scale decompression products in ultra high-pressure phengite: HR-TEM and AEM study, and some petrological implications. *Amer. Mineralogist* 85, 1195–1201.

Geroch S. & Nowak W. 1984: Proposal of zonation for the Late Tithonian–Late Eocene, based upon arenaceous Foraminifera from the Outer Carpathians, Poland. In: Oertli H.J. (Ed.): Benthos' 83: 2nd International Symposium on Benthic Foraminifera (Pau, April 11–15, 1983). *Elf-Aquitane, ESO REP and TOTAL CFP*, Pau & Bordeoux, 225–239.

Haczewski G., Bąk K., Kukulak J., Mastella L. & Rubinkiewicz J. (submitted to print): Ustrzyki Górne Sheet (1068) of Detailed Geological Map of Poland, scale 1:50,000. *Państw. Inst. Geol.*, Warszawa.

Hamor G., Steininger F.F., Kojundgieva E., Cicha I., Vass D., Barthelt D., Halmai J., Boccaletti M., Gelati R., Moratti G., Slaczka A., Marinescu F., Berger J.P., Babak E.V., Goncharova I.A., Ilvina L.B., Nevesskaja L.A., Paramanova N.P., Popov S.V., Eremija M. & Marinovich D. 1989: Neogene Palaeogeographic Atlas of Central and Eastern Europe, scale 1:3,000,000. Maps 1–7. *Geol. Inst. Hung. (MÁFI)*, Budapest.

Hatch F.H., Wells A.K. & Wells M.K. 1961: Petrology of the igneous rocks. 12th edition. *Thomas Murby & Co*, London, 1–515.

Hovorka D. & Petrík I. 1992: Variscan granitic bodies of the Western Carpathians — the backbone of the mountain chain. In: Vozár J. (Ed.): The Palaeozoic geodynamic domains of the Western Carpathians, Eastern Alps and Dinarides. *Spec. Vol. IGCP 276*, Bratislava, 57–66.

Koráb T. & Ďurkovič T. 1978: Geology of Dukla Unit (East-Slovakian Flysch). *Geol. Ústav D. Štúra*, Bratislava, 1–144.

Koszarski L., Ślączka A. & Żytko K. 1961: Stratigraphy and palaeogeography of the Dukla Nappe in the Bieszczady Mts. *Kwart. Geol.* 5, 551–578 (in Polish).

Książkiewicz M. 1962: Geological Atlas of Poland. Cretaceous and

Paleogene stratigraphy and facies in the Polish Central Carpathians. *Inst. Geol.*, Warszawa (in Polish, English summary).

Leško B., Nemčok J. & Koráb T. 1960: Flysch of the Užská hornatina Mts. *Geol. Práce, Spr.* 19, 65–85 (in Slovak).

Maniar P.D. & Piccoli P.M. 1989: Tectonic discrimination of granitoids. *Geol. Soc. Amer. Bull.* 101, 635–643.

Moine B. & de La Roche H. 1968: Nouvelle approche du problème de l'origine des amphibolites, à partir de leur composition chimique. *C. R. Acad. Sci.* 267, 20–84.

Morgiel J. & Olszewska B. 1981: Biostratigraphy of the Polish External Carpathians based on agglutinated foraminifera. *Micropaleontology* 27, 1–30.

Olszewska B. 1980: Foraminiferal stratigraphy of Upper Cretaceous and Palaeogene sediments of the central part of the Dukla Unit. *Biul. Inst. Geol. (Warszawa)* 326, 59–107 (in Polish, English summary).

Olszewska B. 1997: Foraminiferal biostratigraphy of the Polish Outer Carpathians: a record of basin geohistory. *Ann. Soc. Geol. Poloniae* 67, 325–336.

Pearce J.A., Harris N.B.W. & Tindle A.G. 1984: Trace element discrimination diagrams for the tectonic interpretation of granitic rocks. *J. Petrology* 25, 956–983.

Petrík I. 2000: Multiple sources of the West-Carpathian granitoids: A review of Rb/Sr and Sm/Nd data. *Geol. Carpathica* 51, 145–158.

Petrík I. & Broska I. 1994: Petrology of two granite types from the Tribec Mountains, Western Carpathians: an example of allanite (+magnetite) versus monazite dichotomy. *Geol. J.* 29, 59–78.

Petrík I. & Kohút M. 1997: The evolution of granitoid magmatism during the Hercynian orogen in the Western Carpathians. In: Grecula P., Hovorka D. & Putiš M. (Eds.): Geological evolution of the Western Carpathians. *Miner. Slovaca — Monograph* 235–252.

Petrík I., Broska I. & Uher P. 1994: Evolution of the West Carpathian granite magmatism: source rock, geotectonic setting and relation to the Variscan structure. *Geol Carpathica* 45, 283–291.

Pitcher W.S. 1982: Granite type and tectonic environment. In: Hsu K.J. (Ed.): Mountain Building Processes. *Acad. Press*, London, 19–40.

Pettijohn F.J. 1975: Sedimentary rocks. *Harper & Row Publishers,* New York, 1–628.

Poller U., Broska I., Finger F., Uher P. & Janák M. 2000: Early Variscan in the Western Carpathians: U/Pb zircon data from granitoids and orthogneisses of the Tatra Mountains (Slovakia). *Int. J. Earth Sci.* 89, 336–349.

Poprawa P., Malata T. & Oszczypko N. 2002: Tectonic evolution of the Polish part of Outer Carpathian's sedimentary basins — constrains from subsidence analysis. *Przegl. Geol.* 50, 1092–1108.

Poprawa T., Malata T., Pécskay Z., Banaś M., Skulich J., Paszkowski M. & Kusiak M. 2004: Geochronology of crystalline basement of the Western Outer Carpathian's sediment source areas — preliminary data. *Mineral. Soc. Pol. Spec. Pap.* 22, 329–332.

Putiš M., Kotov A.B., Petrík I., Korikovsky S.P., Madarás J., Salnikova S.P., Yakovleva S.Z., Berezhnaya N.G., Plotkina Y.V., Kovach V.P., Lupták B. & Majdán M. 2003: Early- vs. late orogenic granitoids relatioships in the Variscan basement of the Western Carpathians. *Geol. Carpathica* 54, 163–174.

Rollinson H. 1993: Using geochemical data: evaluation, presentation, interpretation. *Longman Group UK Ltd.*, London, 1–352.

Simpson C.A. 1985: Deformation of granitic rocks across the brittle-ductile transition. *J. Struct. Geol.* 7, 503–511.

Ślączka A. 1959: Stratigraphy of the Bystre Scale — Middle Carpathians. *Biul. Inst. Geol.* 131, 203–286 (in Polish, English summary).

Ślączka A. 1971: The geology of the Dukla unit — Polish Flysch Carpathians. *Prace Inst. Geol.* 63, 1–167 (in Polish, English summary).

Tompson R.N. 1982: British Tertiary volcanic province. *Scott. J. Geol.* 18, 49–107.

Uher P. & Gregor T. 1992: The Turčok granite — a product of postorogenic magmatism of A-type. *Miner. Slovaca* 24, 301–304 (in Slovak, English summary).

Uher P., Marschalko R., Martiny E., Puškelová Ľ., Streško V., Toman B. & Walzel E. 1994: Geochemical characterization of granitic rock pebbles from Cretaceous to Paleogene flysch of the Pieniny Klippen Belt. *Geol. Carpathica* 45, 171–183.

Winkler W. & Ślączka A. 1992: Sediment dispersal and provenance in the Silesian, Dukla and Magura flysch nappes (Outer Carpathians, Poland). *Geol. Rdsch.* 81, 371–382.

Winkler W. & Ślączka A. 1994: A Late Cretaceous to Paleogene geodynamic model for the Western Carpathians in Poland. *Geol. Carpathica* 45, 71–82.